Evaluation of the Voltage Support Strategies for the Low Voltage Grid Connected PV Generators

Erhan Demirok[*]
Student Member

Dezso Sera[*]
Member

Remus Teodorescu[*]
Senior Member

Pedro Rodriguez[**]
Member

Uffe Borup[***]
Member

[*] Aalborg University
Department of Energy Technology
Pontoppidanstraede 101
Aalborg, 9220, Denmark
ede@, des@, ret@et.aau.dk

[**] Technical University of Catalonia
Department of Electrical Engineering
C. Colom 1
Terrassa, 08222, Spain
prodriguez@ee.upc.edu

[***] Danfoss Solar Inverters A/S
Jyllandsgade 28
Sønderborg, 6400, Denmark
uffe.borup@danfoss.com

***Abstract* – Admissible range of grid voltage is one of the strictest constraints for the penetration of distributed photovoltaic (PV) generators especially connection to low voltage (LV) public networks. Voltage limits are usually fulfilled either by network reinforcements or limiting of power injections from PVs. In order to increase PV penetration level further, new voltage support control functions for individual inverters are required. This paper investigates distributed reactive power regulation and active power curtailment strategies regarding the development of PV connection capacity by evaluation of reactive power efforts and requirement of minimum active power curtailment. Furthermore, a small scale experimental setup is built to reflect real grid interaction in the laboratory by achieving critical types of grid (weak and sufficiently stiff).**

***Index Terms*—Reactive power control, LV network, PV integration, distributed inverters, PV capacity of network, voltage rise**

I. INTRODUCTION

To keep grid voltage in the acceptable range, power generation limitation, usage of electrical storage devices, line voltage drop compensator (LDC) and switching capacitor/reactor banks are widely used solutions. However PV inverters can also contribute to grid voltage support. An inverter is able to operate between 0.9 lagging and leading power factors when its capacity is increased by 11% of nominal power. This additional capacity can be implemented by absorbing reactive power from the grid in order to decrease voltage. This effect on the voltage at the PV connection points depend on grid short circuit power, location and capacity of PV inverter. On the other hand, reactive power has less impact on grid voltage regulation than active power for highly resistive LV networks [2].

In the present effort, network-specific or autonomous voltage support strategies are investigated including solutions with low density of signal communication between inverters. A generic and impedance based experimental setup has been also developed in the laboratory in order to demonstrate practical limitations. The most critical experiment is carried out to investigate voltage rise problem on the test setup.

This paper will give first of all, load flow analysis on a typical radial residential LV network for rural area. The impact of active and reactive power variations on grid voltage is compared by sensitivity analysis. After words two different reactive power reference trajectories are distributed to individual PV inverters in the framework of the minimization of total reactive power effort, which means less reactive flow losses and maximization of voltage drop. The lab-scaled distribution network configuration and details of a PV generation plant including active and reactive power regulation is given in the last section.

II. LOAD FLOW STUDY ON A RURAL NETWORK

Overvoltage at any point of feeder and overloading of distribution transformers are the main constraints to integrate more PVs into LV public networks. To mitigate the voltage rise problem, reactive power service of inverters has been proposed recently ([3]-[6]). On the other hand, some studies claim that voltage support is not efficient if it is accompanied by reactive power service in public LV networks [2]. Instead active power management (curtailment) is suggested due to high R/X ratio. Unfortunately, network parameters (short-circuit capacity, cable or overhead lines (OHL), length of feeders) are not unique and it requires a dedicated load flow study for the relevant network in order to find the best strategy. Voltage sensitivity to active and reactive power variations at each bus can be derived for any network by load flow solution. Elements of resultant sensitivity matrices give the most effective places to support voltage by regulating Q

and P at related nodes. In case of grid-connected distributed PV plants, different Q set values can be assigned to individual plants in such a way that grid voltage can be supported within minimum Q effort (minimum line loss). Moreover P-V and Q-V sensitivity matrices can be compared to each other for a specific network to determine which system parameter input (P or Q) has dominant impact on grid voltage.

Load flow is solved by using following two nonlinear equations and using iterative technique of the Newton-Raphson method. The system Jacobian matrix is updated at each iteration and finally voltage sensitivity matrices $\partial|V|/\partial P$, $\partial|V|/\partial Q$ are calculated [7].

$$P_i = |V_i|\sum_{j=1}^{n}|V_j||Y_{ij}|\cos(\theta_{ij}-\delta_i+\delta_j)$$

$$Q_i = -|V_i|\sum_{j=1}^{n}|V_j||Y_{ij}|\sin(\theta_{ij}-\delta_i+\delta_j)$$

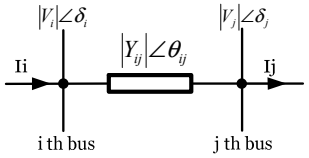

Fig. 1. Load flow solution

A 6-bus rural LV feeder model under certain assumptions is exercised in order to analyze voltage sensitivity to P and Q variations (Fig. 2). Reference paper [3] was used for the typical data of this example network. Regarding the worst case condition of voltage rise problem, consumer load profiles are neglected in this work. Also, the slack bus is assumed to be 1.02 p.u. Base power and base voltage are chosen as 1 MVA and 0.4 kV respectively.

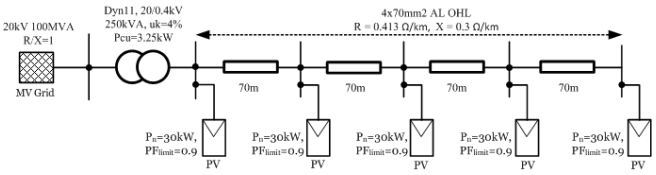

Fig. 2. Example rural LV network for load flow solution

After setting 30-kW active power references for each PV plant with unity power factor and running the load flow code with 4 iterations, the following voltage sensitivity matrices are obtained:

$$\frac{\partial|V|}{\partial P} = \begin{bmatrix} 0.0069 & 0.006 & 0.0056 & 0.0053 & 0.0051 & 0.005 \\ 0.0068 & 0.1917 & 0.1761 & 0.1648 & 0.1576 & 0.154 \\ 0.0067 & 0.1884 & 0.3375 & 0.3196 & 0.3081 & 0.3024 \\ 0.0066 & 0.186 & 0.3331 & 0.4788 & 0.4629 & 0.455 \\ 0.0065 & 0.1843 & 0.3302 & 0.4745 & 0.6217 & 0.6118 \\ 0.0065 & 0.1835 & 0.3287 & 0.4724 & 0.619 & 0.7724 \end{bmatrix}$$

$$\frac{\partial|V|}{\partial Q} = \begin{bmatrix} 0.007 & 0.007 & 0.0071 & 0.0071 & 0.0071 & 0.0071 \\ 0.0068 & 0.3308 & 0.3314 & 0.3317 & 0.3317 & 0.3317 \\ 0.0067 & 0.3252 & 0.4489 & 0.4493 & 0.4494 & 0.4494 \\ 0.0066 & 0.321 & 0.443 & 0.5647 & 0.5649 & 0.5649 \\ 0.0066 & 0.3181 & 0.4391 & 0.5597 & 0.68 & 0.6801 \\ 0.0065 & 0.3167 & 0.4372 & 0.5572 & 0.677 & 0.7966 \end{bmatrix}$$

Diagonal elements correspond to effect of P and Q variation of PV plant on voltage magnitude at the same bus. Two issues can be inferred from above voltage sensitivity matrices:

- Voltage sensitivity for both P and Q variations are increasing as going away from the transformer. It has the highest sensitivity at the end of feeder.
- Reactive power impacts node voltages more than that of active power due to reactance contribution by the transformer (R_{tr}=8.32 mΩ, X_{tr}=24.21 mΩ).
- In addition to the transformer impedance, OHL also plays an important role here on network reactance.

If OHL is replaced with NAYY 4x95mm^2 underground cables (R_{cable}=0.32Ω/km, X_{cable}=0.082Ω/km), new voltage sensitivity matrices become as following

$$\frac{\partial|V|}{\partial P} = \begin{bmatrix} 0.0069 & 0.006 & 0.0057 & 0.0056 & 0.0055 & 0.0054 \\ 0.0068 & 0.1912 & 0.1833 & 0.1776 & 0.174 & 0.1721 \\ 0.0067 & 0.1885 & 0.3102 & 0.3017 & 0.2961 & 0.2934 \\ 0.0066 & 0.1865 & 0.3069 & 0.4271 & 0.4196 & 0.416 \\ 0.0066 & 0.1852 & 0.3048 & 0.4241 & 0.5448 & 0.5402 \\ 0.0065 & 0.1845 & 0.3037 & 0.4226 & 0.5429 & 0.6664 \end{bmatrix}$$

$$\frac{\partial|V|}{\partial Q} = \begin{bmatrix} 0.007 & 0.007 & 0.007 & 0.007 & 0.007 & 0.007 \\ 0.0068 & 0.3297 & 0.3298 & 0.3299 & 0.3299 & 0.3299 \\ 0.0067 & 0.3251 & 0.3586 & 0.3587 & 0.3587 & 0.3587 \\ 0.0066 & 0.3217 & 0.3549 & 0.388 & 0.388 & 0.388 \\ 0.0066 & 0.3194 & 0.3524 & 0.3853 & 0.4181 & 0.4181 \\ 0.0066 & 0.3183 & 0.3511 & 0.3839 & 0.4166 & 0.4493 \end{bmatrix}$$

Now, the active power variation has more impact than that of reactive power on grid voltage as expected. For PV systems connected to LV networks, active power is not managed currently to support grid voltage without storage system. However the reflection of MV grid codes into LV grid standards with integration of generating plants is being discussed to allow distributed network operators (DNOs) to set active power curtailment for individual generating plants. If a PV inverter is desired to be operated in any network flexibly, then both active and reactive power managements can be suggested as additional functions in inverters.

III. Evaluation of Voltage Support Strategies

In this section, MV grid at the feeder model which is depicted in Fig. 2 is composed of an ideal voltage source and short circuit impedance. Bus 1 is located between them and

accordingly bus 7 is assigned to the end of feeder. OHL is utilized for the lines here and service lines from buildings to the feeder connection point are neglected. It is also assumed that all PV modules get the same irradiation level. So, PV capacity is determined such that the set values for active power are increased equally among 5 PV plants by satisfying following constraints: Maximum RMS line-to-line voltage of bus 7 is 1.1 p.u. [8] and maximum loading of the transformer is maintained at 150% of the nominal apparent power [9].

Base case:

As a base case, injection capacity is *30kW/each unit* and all inverters operate at unity power factor (PF) by keeping voltage in safety range (Fig. 3). Although the transformer is not fully loaded in this condition, overvoltage at bus 7 limits the PV injection capacity.

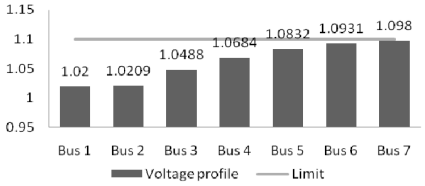

Fig. 3. Base case for distributed reactive set and voltage limit

Strategy 1:

This strategy aims to maximize voltage drop in such a way that individual inverters absorb reactive power at their maximum PF limit of 0.9 as seen from Fig. 4. Regarding of above two network constraints, injection capacity increases to *67.5kW/each unit*. Unlike base condition, 150% transformer loading limits the PV injection capacity here.

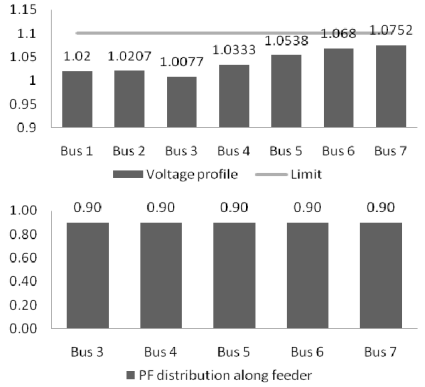

Fig. 4. PF and voltage profile results for Strategy 1

Strategy 2:

If inverters do not need to operate at their reactive power limits ($PF>PF_{lim}=0.9$) during acceptable feeder voltage range, then minimum reactive power consumption can be provided. Since the voltage sensitivity to Q increases as moving away from the transformer, the inverter connected to bus 3 should consume less reactive power. Accordingly the inverter connected to bus 7 should absorb more reactive power from the grid. Thus, transformer loading is relaxed and more PV injection can be still achieved (*70.7kW/each unit*). Fig. 5 shows resulting PF distribution of Strategy 2. Similar to the Strategy 1, installing more PV is also limited by the transformer overloading condition.

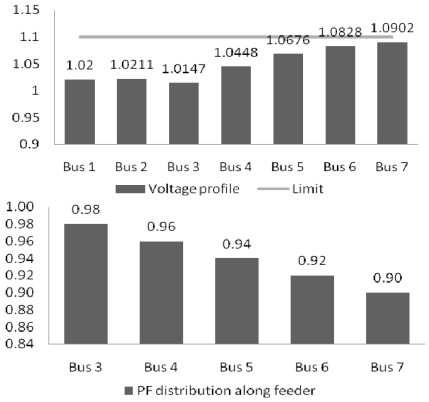

Fig. 5. PF and voltage profile results for Strategy 2

TABLE I
EVALUATION RESULT OF VOLTAGE SUPPORT BY REACTIVE POWER

Strategy No	kW/unit	Total Q consumption [kVAr]	Constraint
Base case	30	0	line overvoltage
Strategy 1 (Min. V_{rise})	67,5	163,46	transformer overloading
Strategy 2 (Min. Q)	70,7	125	transformer overloading

Thus, Strategy 2 corresponds to an optimum solution when the cost of reactive power thereby line losses are considered [10]. However any time Strategy 2 is not sufficient to lower line voltage in admissible range, then Strategy 1 will take over voltage support automatically if all inverters are saturated by their reactive capacity.

Mainly, the droop control and impedance based solutions without any communication infrastructure have been proposed as autonomous operation in order to coordinate and realize PF distribution of Strategy 2.

Droop control is widely used in conventional high-power plants and on DGs connected to islanded networks for power sharing and frequency stability. As depicted in Fig. 6, similar Q=f(U) linear droop curve can also be utilized for individual inverters to coordinate reactive power set values [3]. A dead band which exhibits symmetry on the nominal voltage (1.0p.u.) to the same degree (D) is required to prevent unnecessary Q consumption during operation around nominal voltage.

If short-circuit impedance value at the connection point is measured, then the length of dead band region can be varied adaptively [11]. The inverter located at the end of feeder should start reactive power regulation earlier than the other inverters at the same feeder. Since short-circuit impedance can be interpreted as a measure of distance to the transformer, dead band will become narrower for higher short-circuit impedances (Fig. 7).

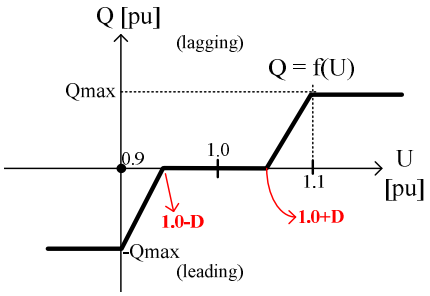

Fig. 6. Q=f(U) droop function

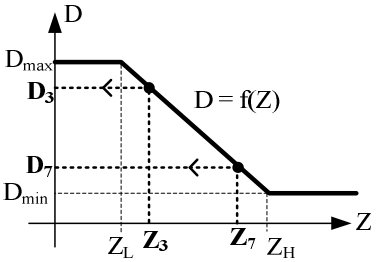

Fig. 7. Impedance based dead band adaption to the droop function

Impedance-adaptive droop function provides flexible PF distribution along the feeder depending on the parameters D_{max}, D_{min}, Z_L and Z_H of D=f(Z) function. These parameters are not network-free but the values can still be selected and classified for the average rural, suburban and urban networks. On the other hand, it is possible that grid impedance measurement techniques with high number of PV inverters running in parallel may interact with each other in fact the precision of impedance measurement is largely influenced unless any synchronization method of signal injections is provided [12].

In another solution, a PF distribution with Strategy 1 is achieved by utilizing low bandwidth communication line [13] (Fig. 8). The method starts with autonomous operation based on local voltage measurement as being done in droop function and then the maximum reactive value between all inverters is passed to individual inverters as new set value. In case of actual reactive power being less than the set value, each controller increases the output reactive power to the maximum value regardless of terminal voltage being in admissible range or not. These increments cause more voltage drop and finally the required maximum reactive set value also results in decaying trend until reaching to admissible feeder voltage range. Voltage drop is maximized but network losses caused by Q flow become higher than the method of impedance-based dead band adaptation.

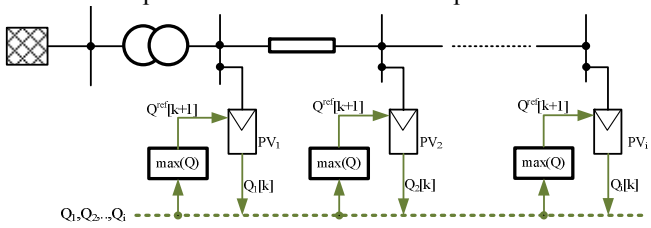

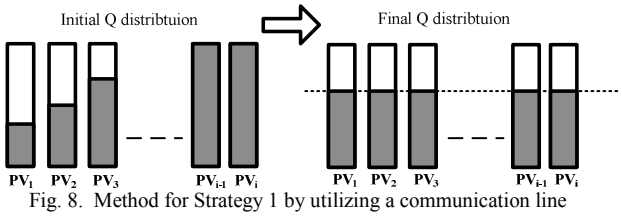

Fig. 8. Method for Strategy 1 by utilizing a communication line

Grid-connected inverters currently include overvoltage protection system which uses a moving 10-minute average voltage. In case of 1.1-p.u. overvoltage condition [8] inverter shall disconnect from grid. Especially during hours with peak irradiation level, total output power loss from PVs will increase and unwanted tripping actions are appeared just after recovery of feeder voltage and so on. As another disadvantage, since available overvoltage protection system measures only local terminal voltage, inverters which are located at the end of feeder will be disconnected first as usual. Before a PV plant is connected to the feeder, this problem can be prevented by simple load flow calculations. Therefore DNO allows only limited amount of integration of PV plants on LV networks by estimating maximum power injections and minimum load demands.

Instead of limiting PV capacity, active power curtailment can be put into use [14], [15] or be additional function to the reactive power service when overvoltage condition is still not removed (Figure 9).

The most critical parameters in Fig. 9 which provide coordination between inverters are the width of dead band in p.u. (D), starting point for power reduction (V_{LP}) and final disconnection point (V_{HP}). V_{LP} and V_{HP} simply determine the P reduction slope (W/V). D may be set fixed for all inverters connected to the same feeder or may be varied for the coordination of reactive power distribution. P=f(V,V_{HP},V_{LP}) and Q=f(V,D,P,PF_{lim}) functions are defined as following

$$P = -\frac{P_{nom}}{V_{HP} - V_{LP}}(V - V_{HP}) \qquad (1)$$

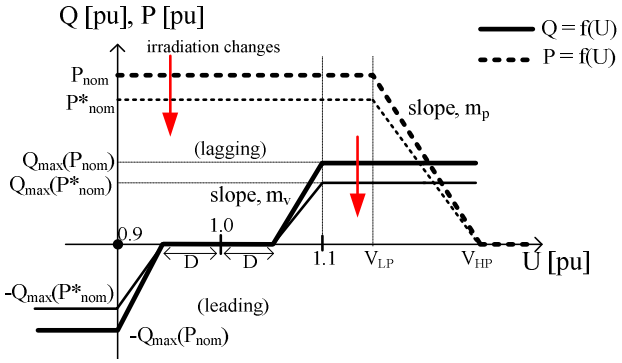

Fig. 9. Reactive and active power managements for grid voltage support

$$Q=\begin{cases}\dfrac{V}{|V|}P.\tan(a\cos(PF_{\lim})), & V<0.9.or.V>1.1\\ 0, & 1-D\le V\le 1+D\\ \dfrac{Q_{\max}}{0.1-D}(V-1-D), & 1+D<V\le 1.1\\ Q_{\max}\left(\dfrac{V-1+D}{0.1-D}\right), & 0.9\le V<1-D\end{cases} \quad (2)$$

where Q_{max} is a function of instantaneous P and power factor limit.

$$Q_{\max}=P.\tan(a\cos(PF_{\lim}))$$

To verify the operation of simple droop functions for both reference generation of reactive and active power curtailment as given in (1) and (2), the same network in Fig. 2 is simulated by a commercial program with the same assumptions (Fig. 10). Each PV inverter is equivalently modeled as current sources with nominal power of 30-kW and limit of 0.9 power factor. Relevant model blocks for each plant are similar and illustrated in Fig. 11. A first-order lag element PT1 should be applied after power references in order to make sharp references slow down and accordingly local oscillations caused by iterative interactions of P and Q can be damped.

30-kW constant set values at unity power factor are assigned to PV inverters during RMS simulation. Slack bus voltage is chosen as 1.06 p.u. to force PV inverters work in P curtailment mode. Critical parameters are also fixed as D=0.05 p.u., V_{LP}=1.11 p.u. and V_{HP}=1.15 p.u. P and Q

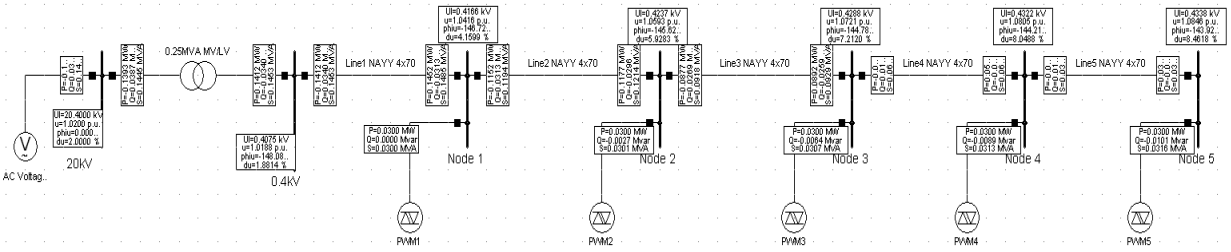

Fig. 10. Simulation of distributed PV inverters

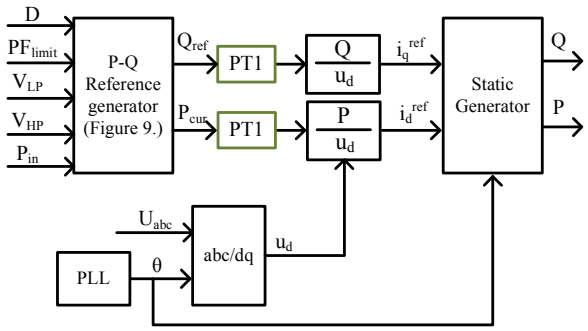

Fig. 11. Model blocks for each distributed plant

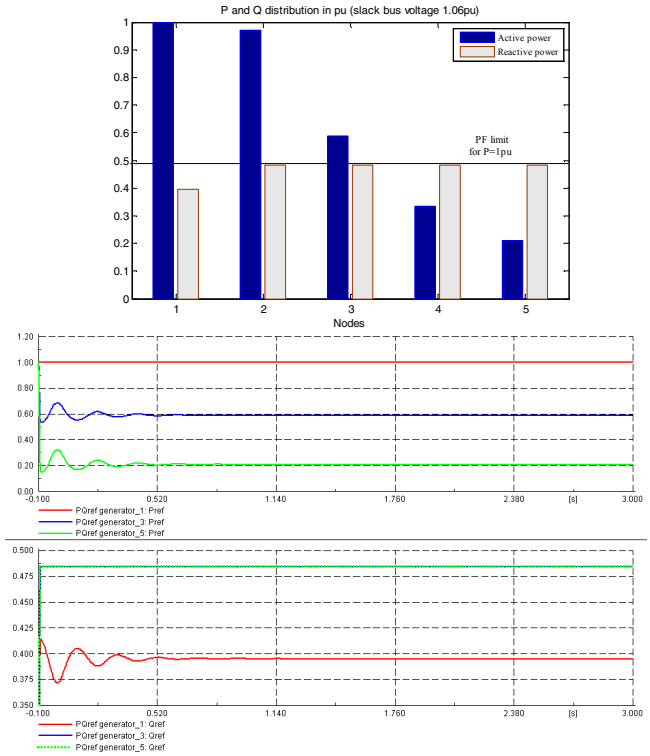

Fig. 12. Offline operation results of Fig. 9 without PT1

reference generator block is first operated as offline to verify (1) and (2). Steady state power reference generations for PV1, PV3, PV5 and corresponding time scale results without PT1 are shown in Fig. 12. The last three inverters operate at their reactive limits and try to apply optimal reactive distribution of Strategy 2 in the feeder. Since P curtailment function (1) simply relies on local voltage measurement, unfair P distribution is resulted in spite of getting the same level irradiation.

A similar approach with adaptive D is proposed in [16] and [17] by measuring only local output current and voltage. However unfair distribution of active power is still maintained. Two alternative solutions can improve the available techniques:

- Q equalization technique with a communication line which is depicted in Fig. 8 can be also applied for P equalization.
- V_{LP} parameter can be also changed adaptively.

IV. Demonstration of Lab Setup for Developing Voltage Support Strategies

In this section, a small scale experimental setup to reflect real grid interaction on the laboratory conditions with three 3.4-kVA inverters is introduced and outcomes of the setup will be supported in the future. The following topics should be able to be investigated with the setup:

- Voltage rise problem and voltage support coordination between inverters.
- Network impedance with multiple inverters
- Voltage unbalance correction
- Operation and support under grid faults
- Investigation and compensation of fast voltage changes at PV connection points due to rapid irradiation changes under different grid types (weak and stiff).

A. *Lab-scaled Distribution Network*

Voltage change at connection point can be estimated easily in terms of short circuit impedance and power supply from DG by simplification of the problem into thevenin circuit (Fig. 13).

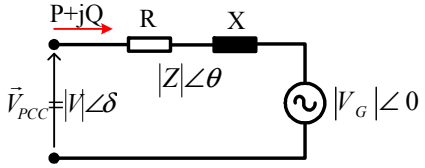

Fig. 13. Thevenin equivalent circuit of connection between generating plant and network

where $\vec{V}_G$ is defined as thevenin grid voltage, R and X are short circuit resistance and reactance respectively. Thus voltage rise is estimated under the following assumptions:

- Grid voltage magnitude is fixed and its phase angle is zero
- Injected active and reactive power are very small (zero) compared to the short circuit power
- Voltage angle at the point of common coupling (PCC) is approximated as zero.

$$\vec{V}_{PCC} \approx |V_G| + \underbrace{\frac{RP+XQ}{|V_G|} + j\left(\frac{XP-RQ}{|V_G|}\right)}_{\Delta\vec{V}_{PCC}} \tag{3}$$

Approximation becomes more accurate solution for the high R/X ratios and low power injections. Equation 3 can also be written in terms of short circuit power

$$\frac{\Delta U}{|V_{PCC}|} = \frac{1}{SCR}[\cos(\varphi-\theta)+j\sin(\theta-\varphi)] \tag{4}$$

for lagging power factor operation. SCR is defined as short circuit capacity ratio (S_{sc}/S_{base}), φ is the phase angle between injected current and terminal voltage, θ is the impedance angle. Thus, suitable impedance values can be calculated in such a way that desired voltage rise is obtained at the end of line. Around 1.1-p.u. voltage rise (Table II) can be achieved with following resistance and reactance values by keeping constant fixed R/X=2.5:

R_1=1Ω, R_2=1.2Ω, R_3=1.5Ω, X_1=0.4Ω, X_2=0.48 Ω, X_3=0.6 Ω

TABLE II
Voltage Rise Emulation at Each Connection Point

Connection points	**A** [ΔV,%]	**B** [ΔV,%]	**C** [ΔV,%]
only PV1	1.438	1.438	1.438
only PV2	1.438	3.203	3.203
only PV3	1.438	3.203	5.419
PV1+PV2+PV3	**4.314**	**7.844**	**10.060**

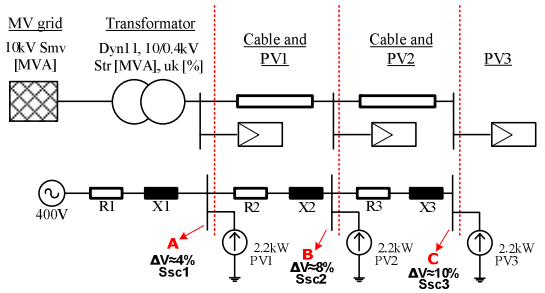

Fig. 14. Single line diagram of lab-scaled distribution network

B. *Details of PV Generator Controller Design:*

The study of voltage support strategies requires stable operation of inner loop controllers. Overall controller scheme used for each 3-phase PV inverter is illustrated in Fig. 15. The inner current loop is regulated by two duplicate proportional+resonant controllers in stationary reference frame. Controller gains are derived according to LCL filter transfer function including time delays and verified in dSpace real time environment. More specific data of each inverter setup is given as:

- Three-phase full-bridge 3.4kVA/2.2kW,
- switching frequency at 8kHz, SPWM+3rd harmonic injection modulation,

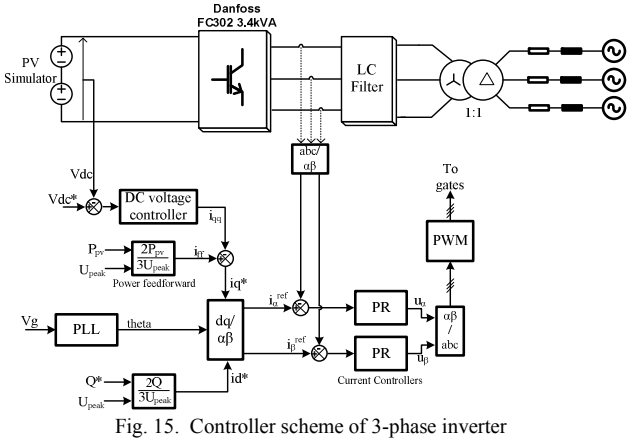

Fig. 15. Controller scheme of 3-phase inverter

- the value of inverter side filter inductance is 6.9mH, filter capacitor is 4.7uF, transformer leakage inductance is 2.5mH, and accordingly resonance frequency of the LCL filter is 1.7kHz

Step response result of reactive power with fixed PV power is shown in Figure 16. Inverter under test was connected to laboratory grid which shows highly resistive impedance characteristics and decoupling of active and reactive power is achieved.

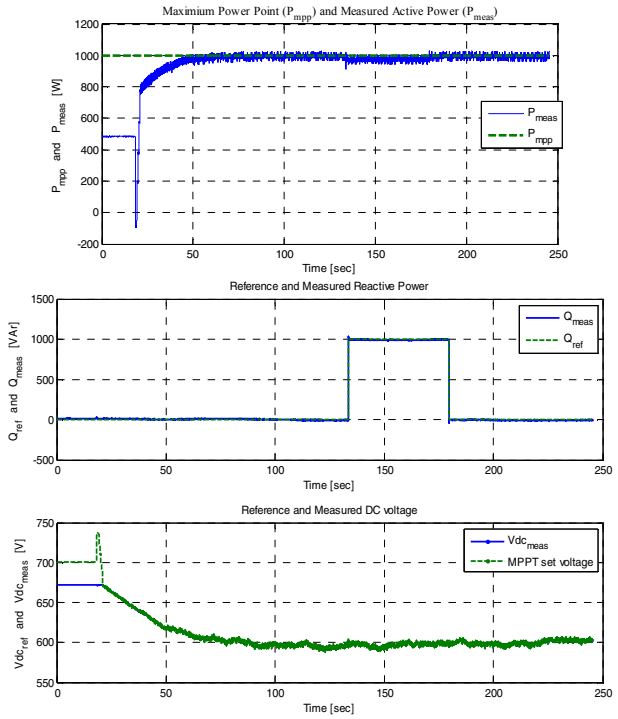

Fig. 16. Experimental results of one PV generator (MPPT is activated at 21st second). P_{mpp}=1kW, V_{mpp}=590V, G=1kW/m^2, DC voltage controller parameter: K_p=0.35, current controller parameters: K_p=12, K_i=3000, Ki_5=Ki_7=1000 (5th and 7th resonant integrator gains)

PV Simulator and MPPT:

As long as values of open circuit voltage, maximum power point voltage/current, and short circuit current are provided by PV array datasheet, (5) can be implemented with slower task compared to switching frequency of 8 kHz [19].

$$v_{pv} = N_{ps} V_{OC} + N_{ps} * N_S * V_T * \ln\left(1 - \frac{i}{I_{SC,1000}\dfrac{G}{1000}}\right) \quad (5)$$

where N_{ps} is the number of panels in series, Ns is the number of series connected cells in each panel, V_T is thermal voltage.

PV simulator is built by two identical programmable DC power supplies and MPPT task provides implementation of Perturb-Observation (P&O) method. The sampling frequency of MPPT is selected as 2 Hz and the voltage increment is set to 2 V.

Investigation, Development and Testing of Voltage Support Functions:

Programmable AC power source and AC load are able to simulate grid voltage changes in fast and slow variations (Fig. 17). Thus voltage dependent any functions like different droop characteristics can be investigated and developed. Fig. 18 shows the implementation result of P-Q management with D=0.05, V_{LP}=1.11 p.u., V_{HP}=1.15 p.u., PF_{lim}=0.9 and P=1 kW.

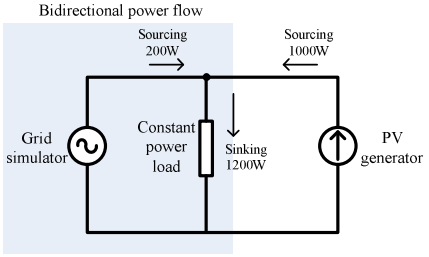

Fig. 17. Investigation and testing of droop functions

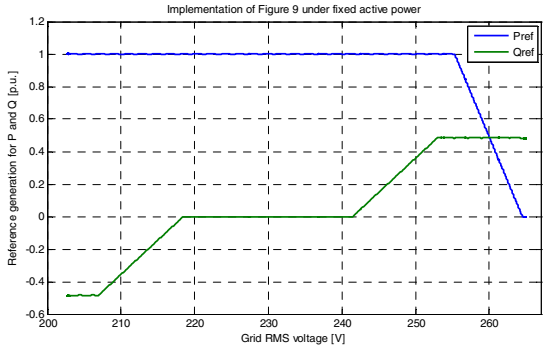

Fig. 18. Implementation result of Fig. 9

V. CONCLUSION

In this study, both active and reactive power effects on feeder voltage are analyzed by voltage sensitivity matrix. Changing line type from OHL to underground cable causes voltage sensitivity to reactive power be reduced as compared to active power. The importance of reactive power service by PV inverters is demonstrated for a rural network and PV capacity can be increased more than 100% of base case. Parameter adaptive and fixed droop-like functions are evaluated for coordination of reactive power support among distributed inverters. Two solutions are proposed in order to improve available techniques. A lab-scaled test setup which reflects real operation as much as possible is introduced as well. Thus decentralized or centralized control of distributed PV inverters including PV dynamics can be developed.

ACKNOWLEDGMENT

This work was supported by the Aalborg University-Danfoss Solar Inverters A/S partnership. Any opinions, findings, and conclusions or recommendations expressed in this material are those of the authors and do not necessarily reflect those of Danfoss Solar Inverters A/S. The authors gratefully acknowledge the contributions of T. Kerekes, M. Altin and O. S. Senturk from Aalborg University on test setup

development and discussions.

REFERENCES

[1] IEA PVPS Task 10 Activity 3.3, "Overcoming PV grid issues in the urban areas", *Report IEA-PVPS T10-06:2009,* October 2009.

[2] R. Tonkoski and L. A. C. Lopes, "Voltage regulation in radial distribution feeders with high penetration of photovoltaic," in *IEEE Energy 2030 Conference,* Atlanta, pp. 1-7, 2008.

[3] M. Braun, T. Stetz, T. Reimann, B. Valov, G. Arnold, "Optimal reactive power supply in distribution networks-Technological and economic assessment for PV systems," in *24th EU PVSEC Conference*, Hamburg, September 2009.

[4] G. Kerber, R. Witzmann, H. Sappl, "Voltage limitation by autonomous reactive power control of grid connected photovoltaic inverters," in *Conference on Compatibility and Power Electronics*, pp. 129-133, May 20-22, 2009.

[5] T. Tran-Quoc, T. M. C. Le, C. Kieny, N. Hadjsaid, S. Bacha, C. Duvauchelle, A. Almeida, "Local voltage control of PVs in distribution networks," in *20nd International conference on Electricity Distribtuion*, Prague, June 2009.

[6] M. Hojo, H. Hatano, Y. Fuwa, "Voltage rise suppression by reactive power control with cooperating photovoltaic generation systems," in *20nd International conference on Electricity Distribtuion*, Prague, June 2009.

[7] H. Saadet, *Power System Analysis*, McGraw-Hill, 1999.

[8] *Voltage Characteristics of Electricity Supplied by Public Distribution Systems*, EN 50160 Standard, 1999.

[9] G. Kerber, R. Witzmann, "Loading capacity of standard oil transformers on photovoltaic load profiles," in *World Renewable Energy Congress (WRECX),* pp. 1198-1203, Glasgow, July 2008.

[10] M. Braun, "Reactive power supply by distributed generators," in *IEEE PES General Meeting-Conversion and Delivery of Electrical Energy in the 21st Century,* pp. 1-8, 2008.

[11] G. Kerber, "Konzept für eine autonome blindleistungsregelung von umrichteranlagen," European Patent EP 1 906 505 A1, April 2008.

[12] A. V. Timbus, R. Teodorescu, F. Blaabjerg, U. Borup, "Online grid impedance measurement suitable for multiple PV inverters running in parallel," in *21st Applied Power Electronics Conference and Exposition (APEC'06)*, 2006.

[13] M. Hojo, H. Hatano, Y. Fuwa, "Voltage rise suppression by reactive power control with cooperating photovoltaic generation systems," in *20th International Conference on Electricity Distribution*, Prague, June 2009.

[14] Y. Ueda, T. Oozeki, K. Kurokawa, T. Itou, K. Kitamura, Y. Miyamoto, M. Yokota, H. Sugihara, S. Nishikawa, "Analytical results of output power restriction due to the voltage increasing of power distribution line in grid-connected clustered PV systems," in *31st IEEE Photovoltaic Specialists Conference*, 2005.

[15] E. Demirok, D. Sera, R. Teodorescu, P. Rodriguez, U. Borup, "Clustered PV inverters in LV networks: An overview of impacts and comparison of voltage control strategies," in *IEEE Electrical Power and Energy Conference (EPEC2009)*, October 2009.

[16] T. Tran-Quoc, T. M. C. Le, C. Kieny, N. Hadjsaid, S. Bacha, C. Duvauchelle, A. Almeida, "Local voltage control of PVs in distribution networks," in *20th International Conference on Electricity Distribution*, Prague, June 2009.

[17] G. Rami, "Controle de tension auto adaptatif pour des productions decentralisees d'energies connectees au reseau electrique de distribution," Ph.D. dissertation, Inst. National Polytechnique de Grenoble, 2006.

[18] E. Demirok, "State of the art analysis for grid interactive PV inverters in LV networks", Aalborg University, Aalborg, DK, Tech. Report.

[19] D. Sera, T. Kerekes, R. Teodorescu, F. Blaabjerg, "Improved MPPT method for rapidly changing environmental conditions," in *IEEE International Symposium on Industrial Electronics,* vol. 2, pp. 1420-1425, July 2006.